STUDYING THE EFFECT OF TRANSPORT LAYERS ON ZrS2/MEH-PPV SOLAR CELLS: USING SCAPS -1D SOFTWARE

Marwan S. Mousa[a], Hmoud Al-Dmour[b]*, Emad K. Jaradat[c], Osama Y. Al-Madanat[d], Ahmad M.D. (Assa'd) Jaber[e], Beddiaf Zaidi[f], Ahmet Sait Alali[g], V. Aravindan[h]

[a]Department of Renewable Energy Engineering, Jadara University, Irbid 21110, Jordan
[b]Department of Physics, Faculty of Science, Mu'tah University, Mu'tah 6170, Jordan
[c]Department of Physics, Faculty of Science. Imam Mohammad Ibn Saud Islamic University, Riyadh 11623, Saudi Arabi
[d]Department of Chemistry, Faculty of Science, Mu'tah University, Mu'tah 6170, Jordan
[e]Department of Basic Humanities and Science, Faculty of Medicine, Aqaba Medical Sciences University, Aqaba 77110, Jordan
[f]Department of Physics, Faculty of Material Sciences, University of Batna 1, Batna, Algeria
[g]Department of Physics, Yıldız Technical University, Istanbul, 34220 Turkey
[h]Smart Materials Lab, Department of Physics, Thiagarajar College of Engineering, Madurai-625015, India
*Correspondence Author e-mail: hmoud79@mutah.edu.jo

This study investigates the effect of charge transport layers on the efficiency of Poly[2-methoxy-5-(2-ethylhexyloxy)-1,4-phenylenevinylene] (MEH_PPV) and Zirconium Disulfide (ZrS2) solar cells using Scaps-1D software. It was found that by increasing the MEH-PPV thickness and decreasing its acceptor doping concentration, the efficiency ($\mu\%$), fill factor (FF), and short-circuit current density (J_{sc}) decreased. Conversely, increasing the thickness of the ZrS2 electron transport layer and decreasing its donor doping density enhanced the efficiency ($\mu\%$) and short-circuit current density (J_{sc}) while maintaining a constant open-circuit voltage (V_{oc}). These results can be attributed to decreased charge separation and collection in MEH-PPV and reduced optical path length in ZrS2. On the other hand, the back contact with work function is below 4.65 eV, the MEH-PPV/ZrS2 solar cells produced the lowest efficiency compared to different types of back contact. Under optimal conditions, MEH-PPV/ZrS2 solar cell shows a high efficiency of 21% when the dopant concentration of MEH-PPV and the value of the neutral defect density at the ZrS2/ MEH-PPV interface are $10^{22}\,cm^{-3}$ and $10^9\,cm^{-3}$ respectively.

Keywords: *SCAPS simulation; Solar cells; Doping density; Interface Defect; Work function*
PACS: 28.41.Ak, 88.40.H, 61.72.Vv,71.55.−I, 73.30.+y

1. INTRODUCTION

Over the past decade, scientists working on solar cells have explored various materials and techniques to create solar cells that are both highly efficient and cost-effective [1–4]. One notable development is perovskite solar cells (PSCs), which have garnered significant attention due to their impressive power conversion efficiency (PCE) and their ability to address several existing limitations [1, 2]. In 2009, Tsutomu Miyasaka and his team published an article demonstrating the achievement of 3.8% power conversion efficiency through a perovskite solar cell with a scaffold of mesoporous TiO2 [3]. Since then, the efficiency of PSCs has rapidly increased to reach 25%, providing an alternative solar cell technology to the Si, CdTe, and copper indium gallium commercial solar cells [2]. In general, solar cells are mainly composed of different materials that work as electron and hole transport layers (ETL, HTL). ETL materials can be prepared from different materials, such as transition metal dichalcogenides (TMDCs) [5, 6]. For example, ZrS2 is a two-dimensional (2D) transition metal disulfide synthesized as a thin film for application in flexible transparent devices. It has high electron mobility and a small energy gap. Therefore, they received significant attention due to their potential as candidates for various applications, including solar cells. In our recent publication, zirconium disulfide (ZrS2) has been used in studying the properties of Go/ZrS2 solar cells. The device shows a high efficiency of 15% [6]. For hole transport materials (HTL), organic materials have been widely used as HTL in fabricating organic light-emitting diode OLEDs or flexible and lightweight organic photovoltaics, in addition to their easy fabrication features [7–9]. One example of such materials is MEH PPV (poly[2-methoxy-5-(2-ethylhexyloxy)-1,4-phenylenevinylene]), which has the absorption of light at a wavelength of 450–550 nm and orbital energy at 5.3 eV for the highest occupied molecular orbital (HOMO) and the lowest unoccupied molecular orbital (LUMO) at 3.2 eV [10]. Moreover, the MEH-PPV layer is interesting for light energy harvesting because it absorbs light in the 450–550 nm range, which has relatively high photon energy and converts more sunlight into electricity [11, 12].

The performance of MEH-PPV solar cells is influenced by the characteristics of the MEH-PPV layer, including its thickness, energy band gap, stability, and mobility [12, 13]. Optimizing these conduction properties is crucial for enhancing the efficiency of organic solar cells. For instance, our previous research illustrates how the traits of nc-TiO2 grains impact the performance of organic-inorganic solar cells and how the rigidity of the thiophene ring affects dye-sensitized solar cell efficiency [14]. The findings indicate that the film morphology developed during processing and the structure of the polymeric chain can hinder the pore filling of the mesoporous layer, which in turn significantly impacts

inter-chain hopping and overall device performance. This study intends to explore the elements that may influence the performance of ZrS$_2$/MEH-PPV by utilizing the capacitance simulator (SCAPS-1D) version 3.3.0, a software tool developed by Burgelman et al. [15]. The factors considered include temperature fluctuations, variations in layer thickness, doping levels, and series resistances of the solar cell components.

2. DEVICE SIMULATION

It has been known that numerical simulation can play a vital role in optimizing different structures of solar cells, such as SCPAS. In the beginning, this simulation was used to simulate the efficiency of solar cells whose components are CuInSe2 and the CdTe family [11]. Then, it was applied to identify the parameters that influence the performance of solar cells. These parameters include the thickness, energy band gap, and charge carrier concentration of components of solar cells. On the other hand, the results obtained from both the SCAPS-1D program and experimental measurements are very close to each other. [16]. The SCAPS-1D software is based on solving the fundamental semiconductor equations essential for modelling solar cell behavior. These include the Poisson equation e, the Poisson equation (1), and the continuity equations for electrons and holes (2 and 3). [6.11]

$$\frac{d^2\psi}{dx^2} + \frac{q}{\varepsilon}\left[p(x) - n(x) + N_D - N_A + \rho_p - \rho_n \right] = 0 \tag{1}$$

$$\frac{1}{q}\frac{dJ_P}{dx} = G_{op} - R(x) \tag{2}$$

$$\frac{1}{q}\frac{dJ_n}{dx} = -G_{op} + R(x) \tag{3}$$

Where ε represents the dielectric constant, q denotes the charge of an electron, NA and ND indicate the densities of ionized acceptors and donors, respectively, Ψ refers to the electrostatic potential, Jp is the current density associated with holes, Jn is the current density associated with electrons, G$_{op}$ signifies the rate of carrier generation, R is the overall recombination rate, p represents the density of free holes, n stands for the density of free electrons, while ρp and ρn are the distributions of holes and electrons, respectively.The following drift-diffusion equations (2) and (3) represent the hole and electron carrier transport properties of the semiconducting material. In this work, the proposed solar cell is composed of zirconium disulfide (ZrS$_2$) and poly[2-methoxy-5-(2-ethylhexyloxy)-1,4-phenylenevinylene] (MEH-PPV) and front contact (fluorine-doped tin dioxide, SnO$_2$;Fn) and back contact (Gold, Au). We studied the dependence of the parameters of solar cells on the properties of charge transport layers. These parameters are power conversion efficiency (μ%), short circuit current density (J$_{sc}$), and fill factor (FF) extracted by drawing the current density versus voltage of solar cells under different conditions and back contact (Gold, Au). Figure 1 shows schematic diagrams of SnO$_2$:F/ZrS$_2$/MEH-PPV/Au solar cells. From previous literature (6,13,17), Tables 1 and 2 present the input parameters used in SCAPS simulators for studying the performance of solar cells.
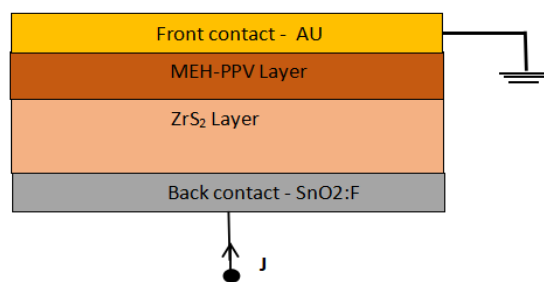

Figure 1. Schematic diagrams of SnO2:F/ZrS$_2$/MEH-PPV/Au solar cells

Table 1. Simulation parameters of components of MEH-PPV/ZrS solar cells

| Material properties	ZrS$_2$	MEH-PPV
Thickness(μm)	Varying	Varying
Bandgap (eV)	1.55	2.1
Electron affinity(eV)	4.7	2.8
Dielectric permittivity(relative)	16.4	3
CB effective density of states (1/cm^3)	2.2 e^{+19}	2e^{+19}
VB effective density of states (1/cm^3)	1.8 e^{+19}	2e^{+19}
Electron mobility (cm^3/Vs)	300	1e^{-5}
Hole mobility (cm^3/Vs)	30	1e^{-6}
Shallow uniform donor density ND (1/cm^3)	1.00 e^{+19}	0
Shallow uniform acceptor density NA (1/cm^3)	0	1e^{18}

Table 2. Simulation parameters of back and front contact of solar cells

Parameters	Back contact (Au electrode)	Front contact (SnO$_2$:F electrode)
Surface recombination velocity of electrons (cm/s)	$1.00E^{+5}$	$1.00E^{+5}$
Surface recombination velocity of holes (cm/s)	$1.00E^{+7}$	$1.00E^{+7}$
Metal-work function(eV)	5.1	4.5

3. RESULT AND DISCUSSION
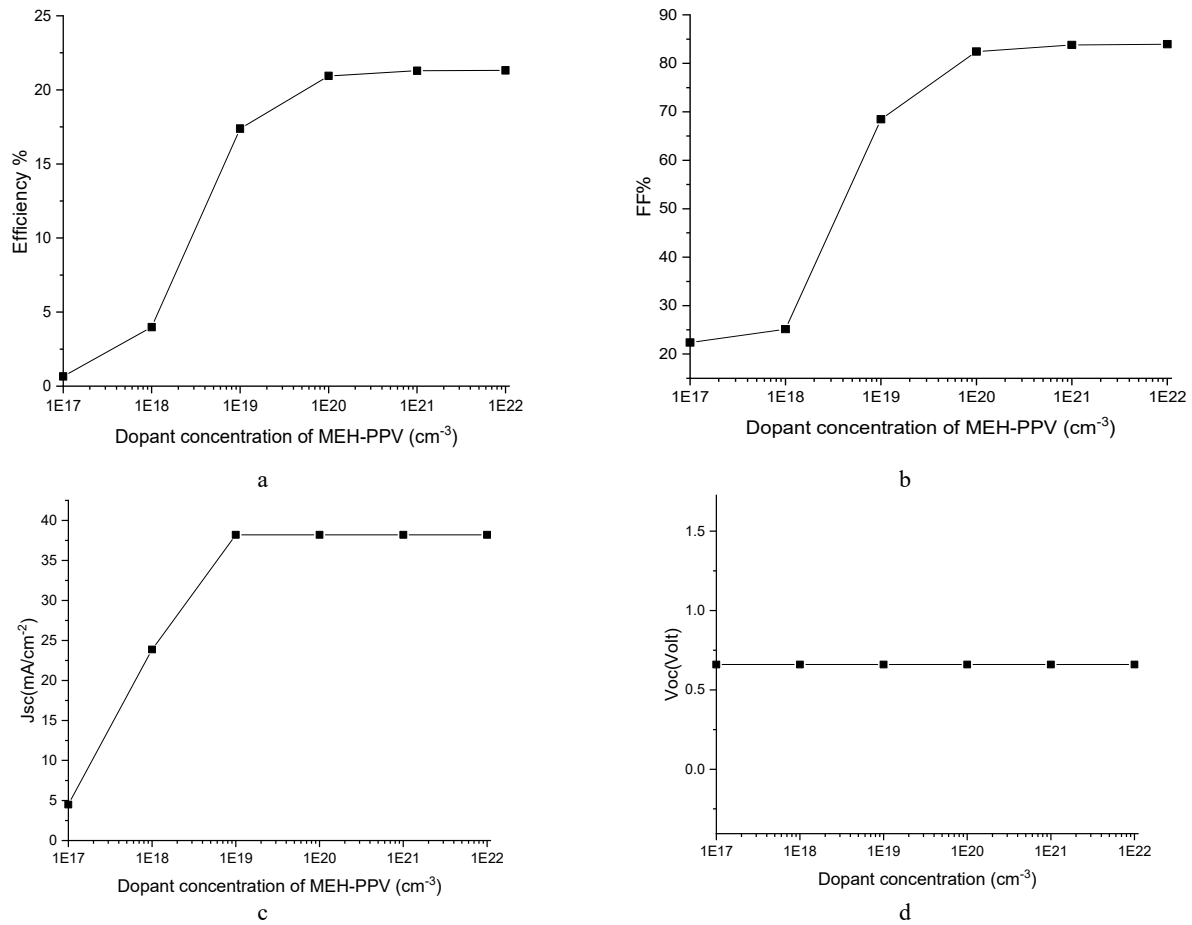### 3.1. Effect properties of MEH-PPV on the performance of solar cells

Figure 2 shows the effect of MEH-PPV thickness on the photovoltaic parameters of MEH-PPV/ZrS$_2$ solar cells. The thickness of the MEH-PPV layer varied from 10 nm to 250 nm.

a

b

c

d
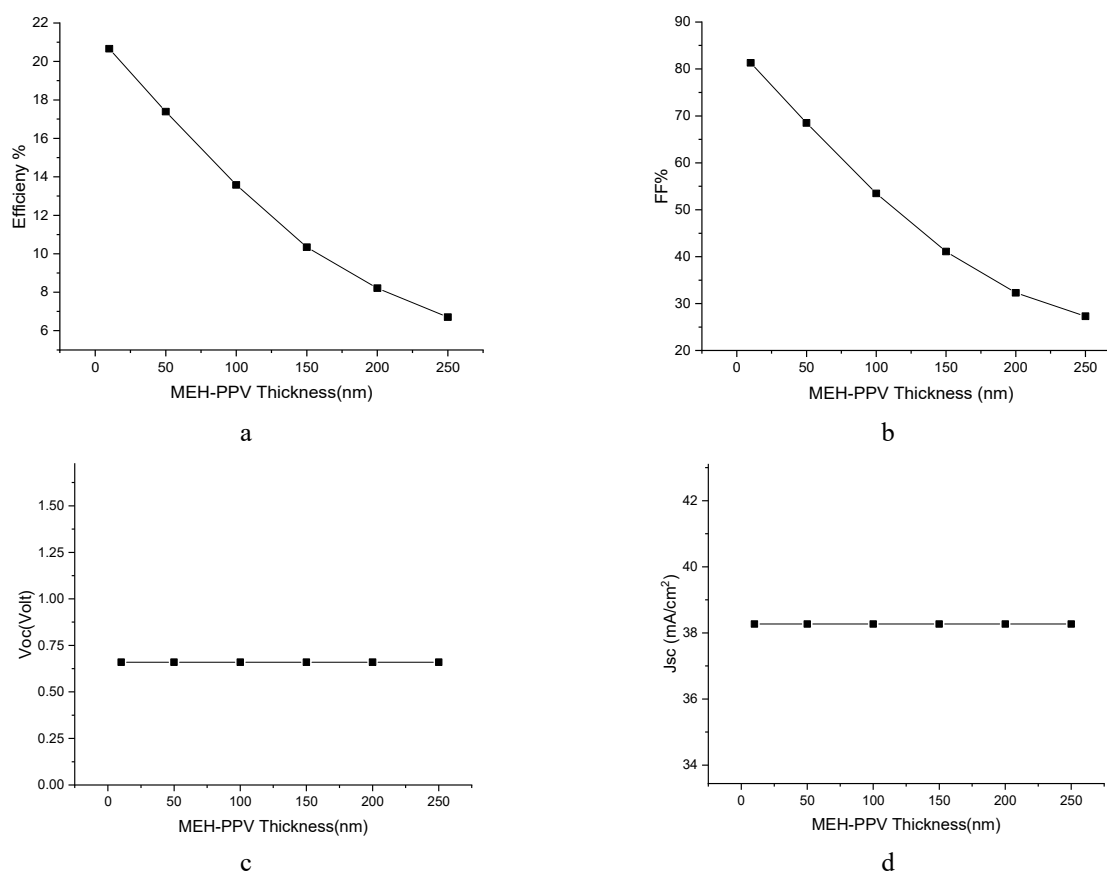
Figure 2. Effect of MEH-PPV thickness on cell performance parameters

Figures 2a and 2b demonstrate that an increase in MEH-PPV thickness from 10 nm to 250 nm results in a decrease in both efficiency and fill factor, from 20.66% to 6.71% and from 81.3% to 27.24%, respectively. This is attributed to reduced charge separation collection at the MEH-PPV and ZrS$_2$ interface due to the bad matching of their atomic orbitals. Besides, thicker HTL in solar cells increases the series resistance in the pathway of positive charge transport additions, which introduces defects and traps, thus, leading to increased charge recombination. These drawbacks cause a decrease in the performance of MEH-PPV solar cells, which agrees with the published work in [18]. On the other hand, Figures 2c and 2d show the open-circuit voltage (V$_{oc}$) and short-circuit current density remain constant at approximately 0.87 V and 32.2 mA/cm², respectively, because the built-in potential is not affected by the increase in thickness.

Figure 3 shows J$_{SC}$, V$_{oc}$, FF, and efficiency of the MEH-PPV /ZrS$_2$ solar cell as functions of the acceptor doping concentration of the MEH-PPPV layer. This concentration was changed over five orders of magnitude from 1×10^{17} to 1×10^{22} cm^{-3}. The results show that the low MEH-PPV doping level produces lower efficiency and fill factor compared to the high MEH-PPV doping level in MEH-PPV/ZrS$_2$ solar cells. Figures 3a and 3b show the efficiency and fill factors were enhanced with an acceptor doping concentration ranging from 0.66% to 21.32% and 22.38% to 83.95%, respectively. Moreover, the open circuit voltage V$_{oc}$ remains constant while the short circuit current density increases and reaches its peak value with an increase in doping density (see Figures 3c and 3d). The JSC gets saturated with small changes when the doping concentration reaches 10^{-20}cm^{-3}. Similar results are reported by Bradeško et al. who emphasized that a high doping level effectively reduces the ohmic losses of the cell and minimizes free carrier recombination by enhancing the electric field in the space charge region [19]. Therefore, increasing the doping level in the active region leads to extra charge carrier generation and also controls the photocarrier transport path, and consequently, it leads to increased

efficiency. A high doping level effectively reduces the ohmic losses of the cell and minimizes free carrier recombination by enhancing the electric field at the space charge region.

Figure 3. Effect of the doping concentration of MEH-PPV on cell performance parameters

3.2. Effect of properties of ZrS₂ on the performance of solar cells

Figure 4 shows the effect of the thickness of the electron transport layer, ZrS_2 on the performance of ZrS_2/MEH PPV solar cells. Its thickness varied from 0.25 μm to 1.5μm and the values of acceptor density and thickness of MEH - PPV are 0.05μm and 10^{+19} cm^{-3} respectively. The enhancement of efficiency is attributed to an increase in short-circuit current density of around 30%, while the decrease in fill factor was approximately 14%. The advantage of having thicker ZrS_2 improves electron-hole pair generation more than their recombination. This can be explained by the high electron mobility in ZrS_2, which minimizes the increase in series resistance in thicker materials [20]. The results present that the increase in thickness of ZrS_2 leads to an increase in Jsc from 30.61 mA/cm^2 to 38.66 mA/cm^2 whereas the V_{oc} remains constant, which in turn enhances efficiency. This can be explained based on the fact that increasing the ZrS_2 layer thickness leads to enhancing the optical path length of the light falling on the device and ionizing more atoms within the materials. This causes the material to produce more electron-hole pairs, corresponding to a large amount of light absorption. Additionally, the narrow bandgaps of the ZrS_2 layer enhance the photo-charge separation and consequently increase the short circuit current density [21]

Figure 5 shows the effect of donor doping concentration in the ZrS_2 layer on the efficiency, V_{oc}, J_{sc}, and FF of the solar cells. The donor density was varied from 1×10^{17} to 1×10^{22} cm^{-3}. At a lower ZrS_2 doping level, the MEH-PPV/ZrS_2 solar cells produced higher short-circuit current density and efficiency compared to a higher ZrS_2 doping level. As shown in Figures 5-a and 5-b, the efficiency and Jsc decrease as the acceptor doping concentration increases, from 38.2 mA/cm^2 to 35.11 mA/cm^2 and from 17.4% to 16.25%, respectively. Moreover, the open-circuit voltage (V_{oc}) remains constant, while the fill factor (FF%) increases and reaches its peak value with increasing doping density (see Figures 5-c and 5-d). The doping concentration influences the electric field and the processes of charge generation, transport, and recombination. For example, a study reported that low dopant concentrations (<10^{20} cm^{-3}) do not significantly affect the parameters of bulk heterojunction cells, whereas higher doping levels decrease efficiency. These results are consistent with our results, which attribute the increased efficiency at low doping concentrations to reduced recombination rates and improved charge carrier mobility, combined with minimized parasitic losses. Additionally, low doping levels enhance the built-in electric field strength, leading to more effective charge separation and collection [22, 23].
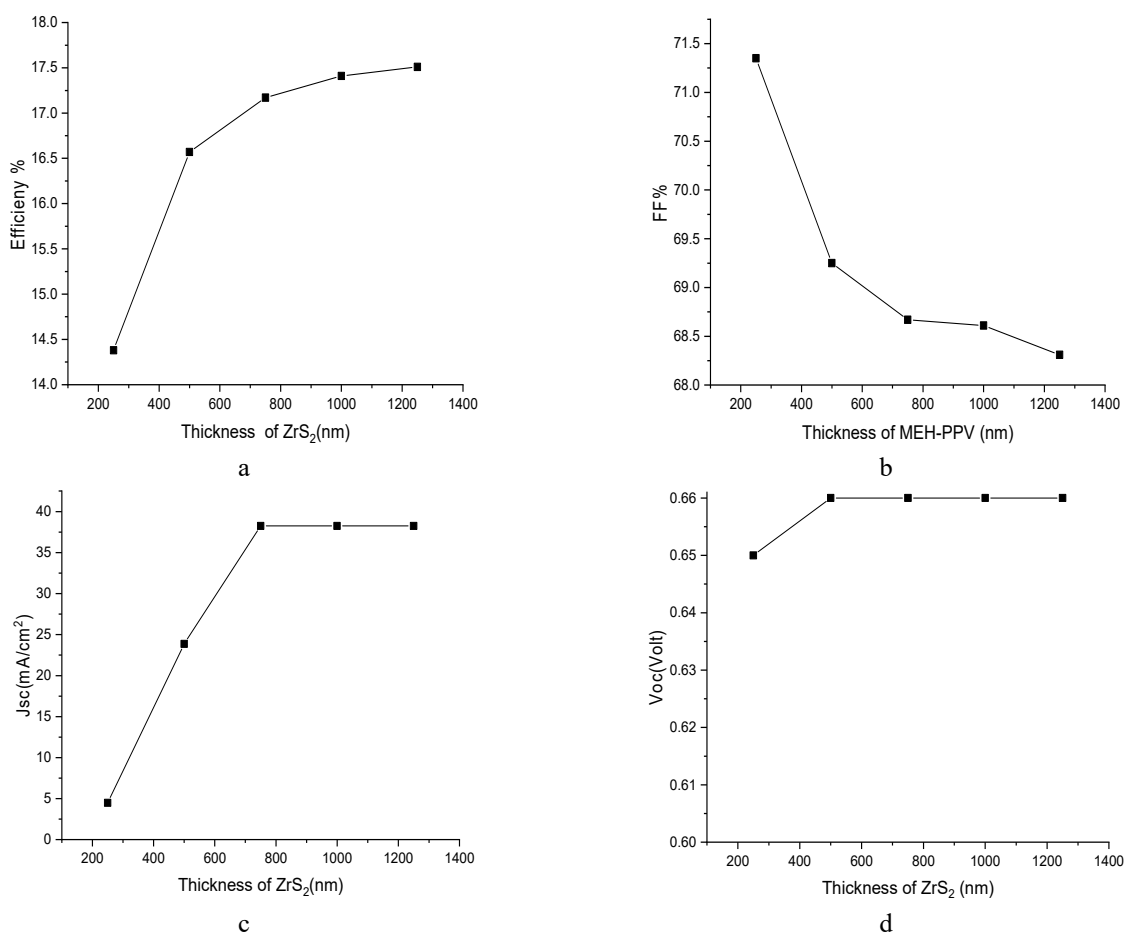
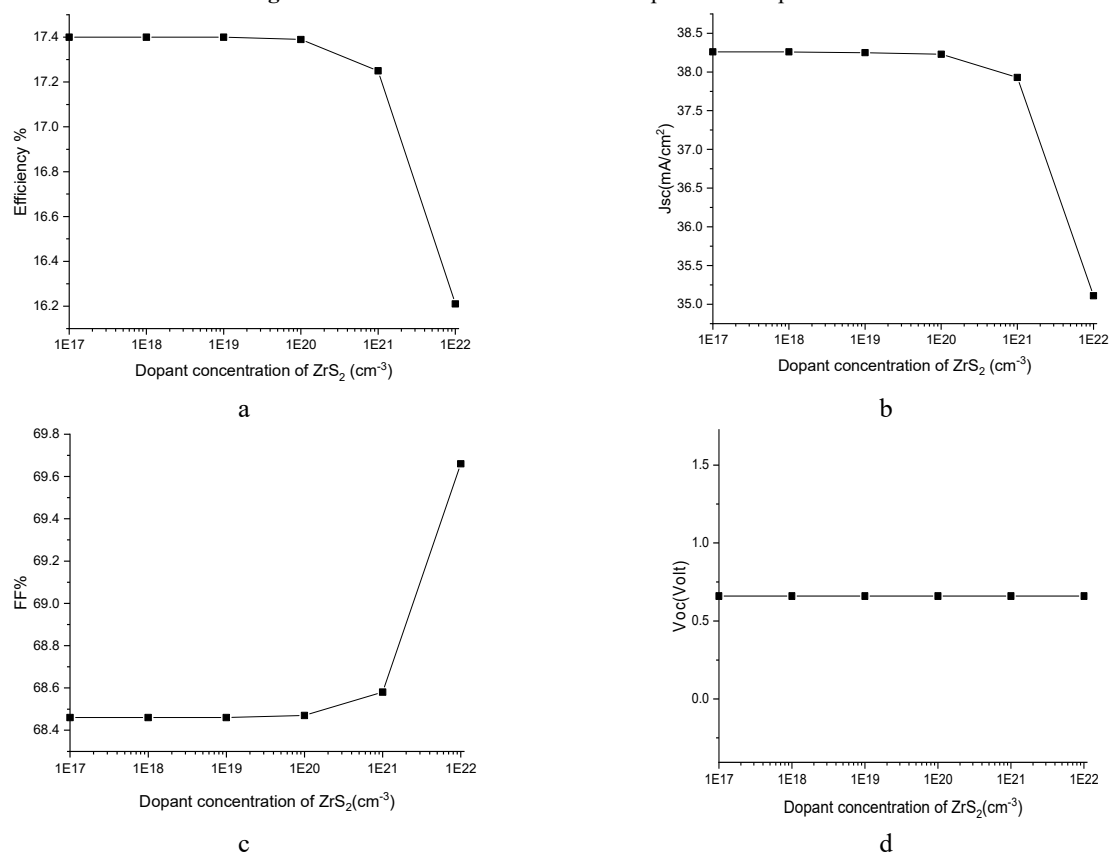**Figure 4.** Effect of ZrS$_2$ thickness on cell performance parameters

Figure 5. Effect of dopin concentration of ZrS$_2$ on cell performance parameters

3.3. Effect of interface defects (N$_{ti}$) on the performance of solar cells

It has been reported that the properties of interfaces play an important role in the permanence of solar cells [24]. In general, the formation of these defects is related to structural imperfections of the active layer, inconsistent fabrication techniques, mismatched energy levels, poor adhesion between ETL and HTL, and exposure to oxygen. In our solar cells, an interface defect is created between ZrS$_2$ and MEH-PPV where charge generation and separation occur. Therefore, to study the influence of defects on a solar cell's efficiency, the neutral defect density at this interface was varied from 1×10^9 cm^{-3} to 10^{15} m^{-3}. Figure 6 shows a reduction in μ, FF, and V$_{oc}$, while J$_{sc}$ remains unaffected by an increase in defect density at the ZrS$_2$/MEH-PPV interface. These results can be attributed to enhanced recombination losses; J$_{SC}$ remains unaffected as it is more dependent on the generation of charge carriers than recombination, which agrees with some of the previous reports [24]. At low defect density, the carrier diffusion length is high, resulting in lower recombination processes, which contributes to improved photovoltaic performance.
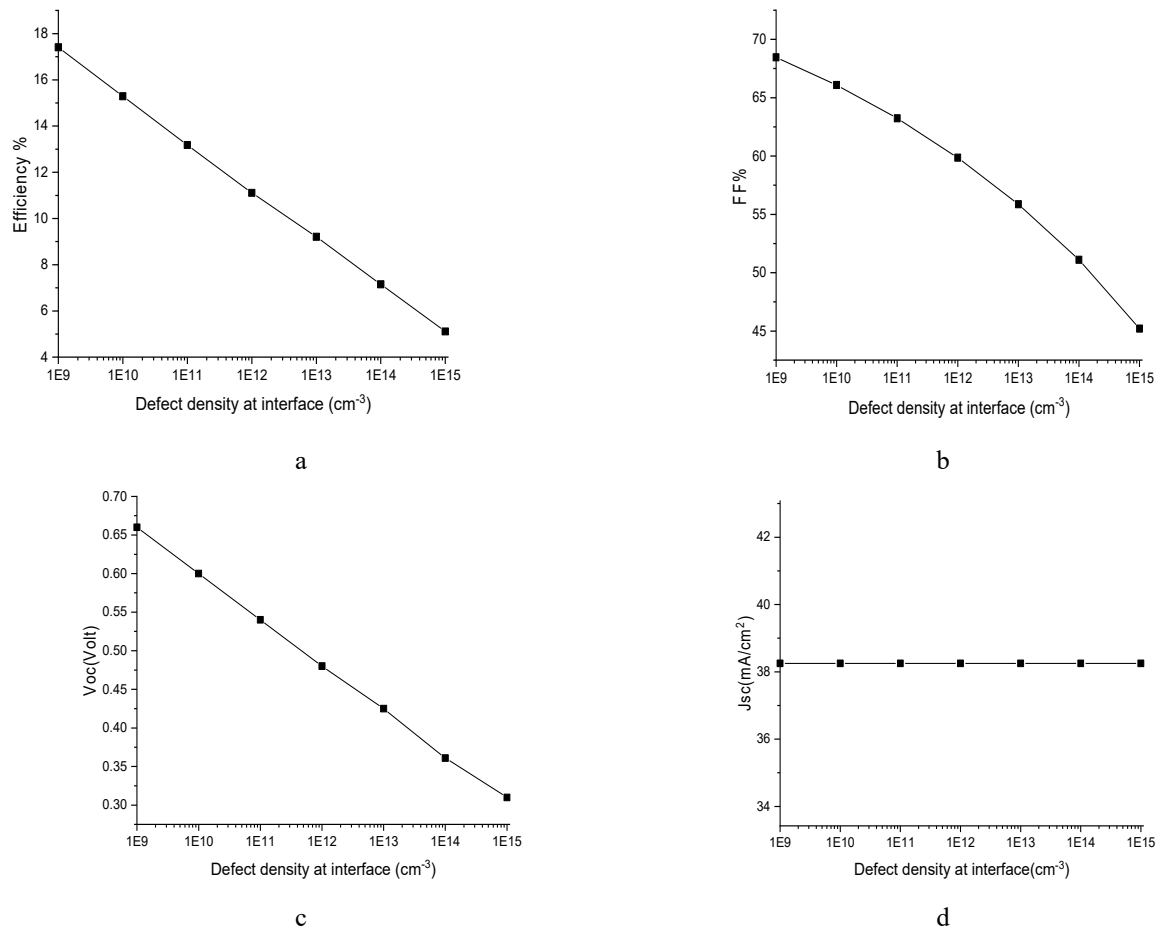

a

b

c

d

Figure 6. Effect of defect density at ZrS$_2$/MEH-PPV interface on cell performance parameters

3.4. Effect of back-contact work function

The properties of back contact in MEH-PPV/ZrS$_2$ solar cells have been studied to enhance their performance and thermal stability. This improvement can be achieved by selecting a suitable work function material as the back contact may yield a reasonable built-in voltage between the metal and active layer. The built-in voltage affects the open-circuit voltage of solar cells, which is accompanied by an increase in electric field. This field within solar cells serves as a driving force for separating and collecting the photogenerated charge carriers from their corresponding electrodes before they recombine and lose. It can also involve selecting appropriate materials with suitable energy levels, modifying the device architecture, or using interfacial layers to adjust the energy level alignment [6]. Table 3 shows the parameters of SnO$_2$:Fn/ZrS$_2$/ MEH-PPV/Au solar cells versus different back-contact work functions. It was observed that with the decreasing of the back contact work function from 5.35 eV to 4.5eV, the V$_{oc}$ stayed constant around 0.66 V. While it reduced to 0.5V when the work function decreased below 4.5 eV. However, both μ and FF continued to decrease from 17.4% to 1.54% and 68.47 to 9.81 respectively. The short circuit current (J$_{SC}$) remained nearly unchanged despite variations in the back contact work function. On the other hand, as the workforce of the back contact decreases, the Schottky barrier at the MEH-PPV/back contact interface increases and impending hole transport from MEH-PPV to the back contact. Consequently, both FF and PCE are also reduced.

Table 3. The parameters of SnO_2:Fn/ZrS_2/MEH-PPV solar cells versus different back-contact metals.

Back contact work function(eV)	Efficiency μ%	FF%	V_{oc}(Volt)	J_{sc}(mA/cm²)
Platinum (Pt) 5.35	17.4	68.47	0.66	38.25
Gold (Au) 5.1	17.4	68.46	0.66	38.25
Copper (Cu) 4.65	12.41	48.85	0.66	38.25
Iron (Fe) 4.5	7.47	29.45	0.66	38.25
Silver (Ag) 4.5	1.54	9.81	0.5	38.1

CONCLUSIONS

This work investigates the effect of properties charge transport layers on performance of MEH-PPV /ZrS₂ solar cells using SCAPS software. The results reveal that Increasing MEH-PPV thickness and decreasing its doping concentration reduce efficiency while increasing ZrS₂ thickness and decreasing its doping density improve efficiency. The optimal values of the neutral defect density interface and the work function of back contact were is 10^9 cm⁻³ and higher 4.65 eV respectively.

ORCID

Hmoud Al-Dmour, https://orcid.org/0000-0001-5680-5703

REFERENCES

[1] N. Kumar, and K. Chandra, Journal of Materiomics, **7**(5), 940 (2021). https://doi.org/10.1016/j.jmat.2021.04.002
[2] S. Liu, V. Biju, Y. Qi, *et al*., NPG Asia Materials, **15**, 1 (2023). https://doi.org/10.1038/s41427-023-00474-z
[3] A. Kojima, K. Teshima, Y. Shirai, and T. Miyasaka, Journal of the American chemical society, 131, 6050 (2009). https://doi.org/10.1021/ja809598r
[4] H. Al-Dmour, R.H. Alzard, R.H.H. Alblooshi, K. Alhosani, S. AlMadhoob, and N. Saleh, Front Chemistry, **7**, 561 (2019). https://doi.org/10.3389/fchem.2019.00561
[5] R. Ranjanm, A. Nikhi, *et al*., Scientific Report, **13**. 1 (2023). https://doi: 10.1038/s41598-023-44845-6
[6] H. Al-Dmour, East European Journal of Physics, (2), 445 (2024). https://doi.org/10.26565/2312-4334-2024-2-58
[7] S. Lee, J. Li, S. Lee, C. Moon, Y. Kim, J. Cao, and C. Jhun, Molecules, **26**(9), 2512 (2021). https://doi.org/10.3390/molecules26092512
[8] W. Brütting, Nature. Material, **18**, 432 (2019). https://doi.org/10.1038/s41563-019-0329-0
[9] S. Al-Taweel, S. Al-Trawneh, H. Al-Dmour, O. Al-Gzawat, W. Alhalasah, and M. Mousa, Heliyon, **9**(10), 21039 (2023). https://doi.org/10.1016/j.heliyon.2023.e21039
[10] R. Suryana, *et al*., IOP Conference series: Materials Science and Engineering, **333**, 012022 (2018). https://doi:10.1088/1757-899X/333/1/012022.
[11] A. Reshak, M. Shahimin, N. Juhari, R. Vairavan, Current Applied Physics, **13**, 1894 (2013). https://doi.org/10.1016/j.cap.2013.07.023
[12] H. Chen, T. Huang, T. Chang, *et al*., Scientific Report, **6**, 34319 (2016). https://doi.org/10.1038/srep34319
[13] R. Chaymaa, *et al*., Matériaux and Techniques, **111**, 507 (2023). https://doi.org/10.1051/mattech/2024003
[14] H. Al-Dmour, S. Al-Trawneh, and S. Al-Taweel, International Journal of Advanced and Applied Sciences **8**(6), 128 (2021). https://doi.org/10.21833/ijaas.2021.06.015
[15] M. Burgelman, P. Nollet, and S. Degrave, Thin Solid Films, **361**, 527 (2000). https://doi.org/10.1016/S0040-6090(99)00825-1
[16] H. Amina, G. Yigit, M. Begrettin, and K. Hamdi, Optical Materials, **121**, 111544 (2021). https://doi.org/10.1016/j.optmat.2021.111544
[17] M. Abdelfatah, A. El Sayed, W. Ismail, *et al*., Scientific Report, **13** 4553 (2023). https://doi.org/10.1038/s41598-023-31553-4
[18] D. Lee, and K. Kim, Nanomaterials, 13, 1848 (2023). https://doi.org/10.3390/nano13121848
[19] A. Bradesko, *et al*., Journal of Material Chemistry, **9**, 3204 (2021). https://doi.org/10.1039/D0TC05854H
[20] A. Mortadi, E. Hafidi, M. Monkade, R. El Moznine, Materials Science for Energy Technologies, **7**, 158-165 (2024). https://doi.org/10.1016/j.mset.2023.10.001
[21] A. Chowdhur, Acta Physica Polonica A, **145**, 215 (2024). https://doi.org/10.12693/APhysPolA.145.215
[22] A. Trukhanov, V. Bruevich, and Yu. Paraschuk, Physical Review B, **84**, 5318 (2011). https://doi.org/10.1103/PhysRevB.84.205318
[23] H. Al Dmour, AIMS Materials, **8**, 261 (2021). https://doi.org/10.3934/matersci.2021017
[24] R. Priyanka, S. Numeshwar, T. Sanjay, and K. Khare, IOP Conf. Series: Materials Science and Engineering, **798**, 012020 (2020). https://doi.org/10.1088/1757-899X/798/1/012020

ДОСЛІДЖЕННЯ ВПЛИВУ ТРАНСПОРТНИХ ШАРІВ НА СОНЯЧНІ ЕЛЕМЕНТИ ZrS2/MEH-PPV: ВИКОРИСТАННЯ ПРОГРАМНОГО ЗАБЕЗПЕЧЕННЯ SCAPS -1D
Марван С. Мусаᵃ, Хмуд Аль-Дмурᵇ, Емад К. Джарадатᶜ, Усама Є. Аль-Маданатᵈ, Ахмад M.D. (Асса'д) Джаберᵉ, Беддіаф Заїдіᶠ, Ахмет Саїт Алаліᵍ, В. Аравінданʰ
ᵃДепартамент інженерії відновлюваної енергетики, Університет Джадара, Ірбід 21110, Йорданія
ᵇДепартамент фізики, факультет природничих наук, Університет Мута, Мута 6170, Йорданія
ᶜДепартамент фізики, природничий факультет. Ісламський університет імама Мохаммада Ібн Сауда, Ер-Ріяд 11623, Саудівська Аравія
ᵈДепартамент хімії, Факультет природничих наук, Університет Мута, Мута 6170, Йорданія
ᵉДепартамент фундаментальних гуманітарних наук і природничих наук, медичний факультет, Університет медичних наук Акаби, Акаба 77110, Йорданія
ᶠКафедра фізики, факультет матеріальних наук, Університет Батна 1, Батна, Алжир
ᵍФакультет фізики, Технічний університет Йилдиз, Стамбул, 34220 Туреччина
ʰЛабораторія Smart матеріалів, факультет фізики, Інженерний коледж Тіагараджар, Мадурай-625015, Індія

У цій роботі досліджується вплив шарів транспортування заряду на ефективність сонячних елементів із полі[2-метокси-5-(2-етилгексилокси)-1,4-феніленвінілену] (MEH_PPV) і дисульфіду цирконію (ZrS$_2$) за допомогою програмного забезпечення Scaps-1D. Було встановлено, що при збільшенні товщини MEH-PPV і зменшенні концентрації його акцепторного допування ефективність (µ%), коефіцієнт заповнення (FF) і густина струму короткого замикання (Jsc) зменшуються. І навпаки, збільшення товщини шару транспортування електронів ZrS$_2$ і зменшення його щільності донорного легування підвищило ефективність (µ%) і щільність струму короткого замикання (Jsc), зберігаючи постійну напругу холостого ходу (Voc). Ці результати можна пояснити зниженим розподілом і збором зарядів у MEH-PPV і зменшеною довжиною оптичного шляху в ZrS$_2$. З іншого боку, зворотний контакт із роботою виходу нижче 4,65 еВ, сонячні елементи MEH-PPV/ZrS$_2$ показали найнижчу ефективність порівняно з різними типами зворотного контакту. За оптимальних умов сонячна батарея MEH-PPV/ZrS2 показує високу ефективність 21%, коли концентрація допанту MEH-PPV і значення нейтральної щільності дефектів на межі ZrS$_2$/MEH-PPV становлять 10^{22} см-3 і 10^9 см$^{-3}$ відповідно.

Ключові слова: *SCAPS моделювання; сонячні елементи; щільність легування; дефект інтерфейсу; робоча функція*